ADVANCED ELECTRONIC MATERIALS
www.advelectronicmat.de

The Influence of Backbone Fluorination on the Dielectric Constant of Conjugated Polythiophenes

Pierre Boufflet, Gianluca Bovo, Luca Occhi, Hua-Kang Yuan, Zhuping Fei, Yang Han, Thomas D. Anthopoulos, Paul N. Stavrinou, and Martin Heeney**

The ability to modify or enhance the dielectric constant of semiconducting polymers can prove valuable for a range of optoelectronic and microelectronic applications. In the case of organic photovoltaics, increasing the dielectric constant of the active layer has often been suggested as a method to control charge generation, recombination dynamics, and ultimately, the power conversion efficiencies. In this contribution, the impact that the degree and pattern of fluorination has on the dielectric constant of poly(3-octylthiophene) (P3OT), a more soluble analogue of the widely studied conjugated material poly(3-hexylthiophene), is explored. P3OT and its backbone-fluorinated analogue, F-P3OT, are compared along with a block and alternating copolymer version of these materials. It is found that the dielectric constant of the polymer thin films increases as the degree of backbone fluorination increases, in a trend consistent with density functional theory calculations of the dipole moment.

1. Introduction

Manipulation of the dielectric constant of conjugated materials through design is an attractive prospect for microelectronic and optoelectronic applications. In the microelectronic arena, several purposes are readily apparent. Enhancing the permittivity of organic dielectric layers in capacitors can lead to enhanced energy storage,[1] while in transistor architectures, an enhanced permittivity can be used to decrease the operating voltage of the gate electrode.[2] In optoelectronics, a pertinent example is the organic photovoltaic device. Increasing the dielectric constant of the active layer has been proposed for increasing power conversion efficiencies.[3–8] Charge recombination is heavily influenced by the dielectric constant of the constituent materials comprising the active layer. Since the exciton binding energy is inversely proportional to the permittivity of the light-absorbing material, dissociation of excitons to form free charges is enhanced in conjugated materials with higher dielectric constants.[9] Bimolecular recombination is also reduced by increasing the dielectric constant of the active layer, as carriers of opposite charges are better screened from each other.[5,10] The decrease in both recombination types can be expected to result in a net increase in charge collection, and consequently short circuit current (J_{sc}). Lower binding energies are also expected to reduce losses in the open-circuit voltage (V_{oc})—another key metric for power conversion efficiency.[6,11,12] Furthermore, lower rates of bimolecular recombination also enhance V_{oc}.[5] Considering the importance of the active layer permittivity on charge generation in organic photovoltaics (OPV), surprisingly few studies investigate the systematic increase of the dielectric constant in active layer components. Since most common conjugated polymers exhibit ε_r values between 2 and 4 and $PC_{71}BM$, the most common fullerene used in OPV has an ε_r of 3.9, the potential for improving the overall dielectric constant of the active layer is significant.[3,13–15]

The desire to control the refractive index of nonconjugated polymers has led to several guidelines for tailoring the refractive index and, by association, the dielectric constant (see e.g., ref [16]). Molar refractions, derived from the Lorentz–Lorenz equation, suggest that large polarizable groups can be introduced into the polymer repeating units in order to increase the refractive index, as is the case for dipolar groups.[16] Interestingly, fluorine has a lower molar refractivity than hydrogen, so fluorination is predicted to lead to a lower refractive index and permittivity. This is evident in comparing polyethylene to its fully fluorinated analogue, which exhibits a substantially lower refractive index.[17] However, partial fluorination can have a different effect since dipoles are introduced in the repeating units. As a result, the permittivity of partially fluorinated polymers can follow a very

Dr. P. Boufflet, Dr. Z. Fei, Dr. Y. Han, Prof. M. Heeney
Department of Chemistry and Centre for Plastic Electronics
Imperial College London
London SW7 2AZ, UK
E-mail: m.heeney@imperial.ac.uk
Dr. G. Bovo, Dr. L. Occhi, H.-K. Yuan, Prof. T. D. Anthopoulos
Department of Physics and Centre for Plastic Electronics
Imperial College London
London SW7 2AZ, UK
Prof. P. N. Stavrinou
Department of Engineering Science
University of Oxford
Parks Road, Oxford OX1 3PJ, UK
E-mail: paul.stavrinou@eng.ox.ac.uk
The ORCID identification number(s) for the author(s) of this article can be found under https://doi.org/10.1002/aelm.201700375.

DOI: 10.1002/aelm.201700375

different trend. Indeed, manipulation of monomer polarity and size, along with chemical crosslinking can lead to very high ε_r values up to 70, as is the case for P(VDF-TrFE-CTFE).[18,19]

Introducing highly polar groups to increase ε_r in conjugated polymers has been an approach favored by some research groups.[7,10,13,20–22] Such efforts have mainly focused on the introduction of the polar groups within the side chains to avoid disturbing the conjugated backbone, and although ε_r increased, the subsequent performance in an OPV was variable, quite likely due to the influence of such polar groups on blend microstructure. An alternative approach has been the blending of higher dielectric additives with the active layer. A range of such additives have been explored. For example, Torabi et al. investigated bilayer devices in which the donor was blended with camphoric anhydride, resulting in an enhancement of permittivity from 4.5 to 10.8.[13,23] Hyperbranching of conjugated backbones has also been suggested to increase the dielectric constant through long-range polaron delocalisation.[24–26]

Fluorination in conjugated polymer backbones has been explored as a route to increase dielectric constant. For example, difluorination of a partially conjugated thermoplastic polymer led to a 10% increase in the dielectric constant.[27] Similarly, two separate studies have shown that partial backbone fluorination of quinoxaline-based conjugated polymers led to substantial increases in permittivity, and in both cases, fluorination drove increased OPV performance.[4,11] In addition to these efforts, backbone fluorination of conjugated polymers is also motivated by factors other than dielectric constant improvements. Stabilization of both the highest-occupied molecular orbital and the lowest-unoccupied molecular orbital through the addition of electron withdrawing fluorine atoms is a common approach to increase the V_{oc}.[28–30] Reductions in recombination (and the subsequent increase in J_{sc}) upon fluorination have also been widely reported, these, however, are often explained by more favorable microstructure and domain compositions of the active layers, or increased polarization of the exciton, which reduces bimolecular and geminate recombination respectively.[28,31–33]

With the high level of interest in backbone fluorination for organic semiconductors and conjugated polymers, we decided to explore the effects of such fluorination on the dielectric constant of the benchmark materials that are poly(3-alkylthiophenes) (P3AT). We recently reported the synthesis and characterization of poly(3-alkyl-4-fluorothiophenes) (F-P3ATs) and observed that F-P3HT, the fluorinated analogue of P3HT exhibits very low solubility due to aggregation, making its processing difficult.[34] We, therefore, opted to investigate the effect of fluorination on the permittivity of the more soluble octyl analogue, F-P3OT. In this contribution, we probe the effect of backbone fluorination by comparing P3OT with F-P3OT, as well as possible effects of asymmetric fluorination through alternating and block copolymers of these thiophene derivatives. We observe that fluorination of the P3OT polymer leads to an increased ε_r from 2.7 to 4.8, and that the substitution pattern has some impact on the extent of this increase.

2. Results and Discussion

2.1. Synthesis

For the preparation of P3OT-*alt*-F-P3OT, we decided to focus upon the Grignard-metathesis (GRIM)[35] polymerization of the dimer **6** for better control of the regioregularity, and to keep residual catalyst and impurities as consistent as possible across the samples investigated. We note that a related material, P3HT-*alt*-F-P3HT, has recently been reported by a similar polymerization.[36] Exploiting the exclusive selectivity for the magnesium/bromine exchange of **3**,[34] monobrominated compound **4** was produced, which was coupled with **2** to yield the head-to-tail bithiophene **5** in moderate yield after purification by reverse-phase chromatography (**Scheme 1**). Subsequent bromination afforded the monomer **6**, which was polymerized using GRIM conditions, similar to the other polymers (**Scheme 2**). P3OT-*alt*-F-P3OT was purified by Soxhlet extraction, washing with methanol, acetone, hexane, and finally chloroform, before extracting with chlorobenzene. The resulting polymer only exhibited a single resonance in the ^{19}F NMR, suggestive of very high backbone regioregularity (see Supporting Information). No peak attributable to a tail-to-tail defect was observed in our case.[36]

The homopolymers P3OT and F-P3OT were synthesized via GRIM polymerization from the activated monomers **8** and **9**, as previously reported (Scheme 2).[34] The polymers were purified by Soxhlet extraction, washing sequentially with methanol, acetone, and hexane (and chloroform for F-P3OT). P3OT was then extracted using chloroform, and F-P3OT with chlorobenzene. P3OT-*b*-F-P3OT was also synthesized by GRIM polymerization, using the method we recently reported, with the more soluble P3OT block grown first from the activated monomer **8** followed by the addition of activated monomer **9** to the P3OT macroinitiator.[37] The polymer was purified by Soxhlet extraction as with P3OT. However, a further wash with dichloromethane was performed before extraction with chloroform in order to remove traces of P3OT homopolymer. The presence of P3OT homopolymer within P3OT-*b*-F-P3OT is typically characterized by melt and crystallization peaks (at 198 and 155 °C, respectively) observed in the differential scanning calorimetry thermograms (see Figure S1, Supporting Information).[37] After purification, ^{1}H NMR analysis showed that the two blocks were of approximately equal length. ^{19}F NMR only afforded a single peak, again suggestive of very high degrees of backbone regioregularity.

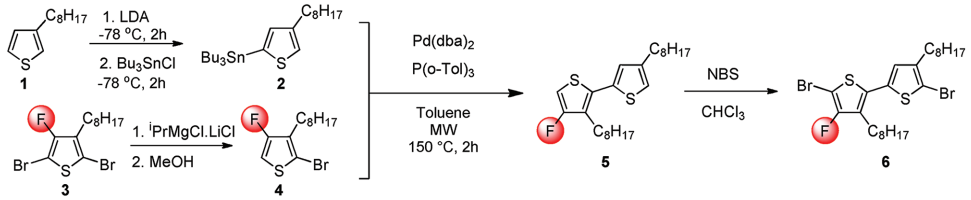

Scheme 1. Synthesis of partially fluorinated bithiophene monomer 6, used in the synthesis of P3OT-*alt*-F-P3OT.

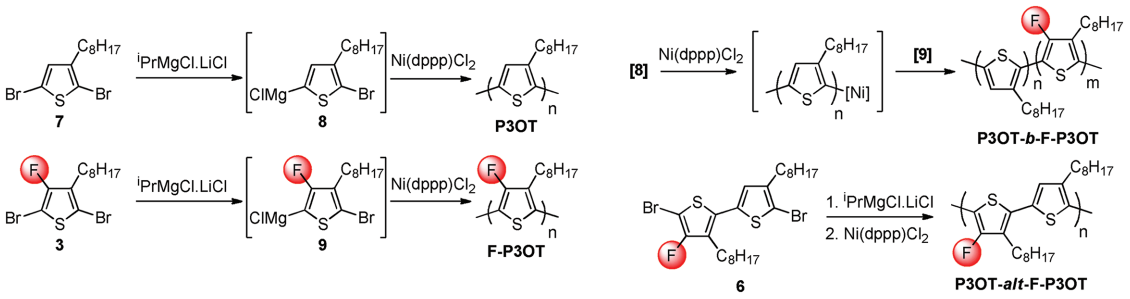

Scheme 2. Synthesis of homopolymers, as well as block and alternating copolymers from GRIM polymerization.

In agreement with our earlier studies,[38] all fluorinated polymers were less soluble than their nonfluorinated analogues and required processing from hot chlorinated solvents like chlorobenzene or 1,2-dichlorobenzene. The molecular weights, as measured by gel permeation chromatography (GPC) in either hot chlorobenzene (P3OT-*b*-F-P3OT and P3OT-*alt*-F-P3OT or hot 1,2,4-trichlorobenzene (F-P3OT), of all fluorinated polymers were similar (**Table 1**).

2.2. Thin-Film Properties

In preparation for the subsequent device studies, the film-forming properties and basic characterization from all four materials were examined. **Figure 1**a shows the absorption spectra, with the absorption coefficients extracted from transmission spectra using the Beer–Lambert expression. All spectra are qualitatively similar, exhibiting a main absorption peak around 530–550 nm, with a clear vibronic progression apparent toward lower energies—a behavior often ascribed to aggregation of the conjugated backbone. The most striking consequence of backbone fluorination is the resulting blue shift of both absorption[34] and emission spectra shown in Figure 1b.

Regarding the absorption coefficient, the P3OT thin film shows the highest value (≈8.3 × 10^4 cm^{-1}). While in comparison, the peak absorption for the fully fluorinated counterpart (F-P3OT) is almost half of this value with the alternating and block copolymers taking on intermediate values. For latter two cases, the P3OT-*alt*-F-P3OT and P3OT-*b*-F-P3OT differ predominantly in the strength of the vibronic structure, with the two main vibronic peaks taking almost equal value in the instance of the alternating compound (P3OT-*alt*-F-P3OT), suggestive of increased interchain coupling and greater backbone planarity—transitioning from H- to J-like aggregation.[39] Interestingly, the peak positions in the absorption profile of P3OT-*b*-F-P3OT appear dominated by F-P3OT contributions despite exhibiting the lower absorption coefficient. This is apparent when comparing the differences between the normalized absorbance spectra of P3OT-*b*-F-P3OT with that obtained from a linear combination of the two constituent polymers, P3OT and F-P3OT (Figure S3, Supporting Information). In common to other di-block polymers, such as thiophene-selenophene-based systems, there is a reasonable match between the spectra and the linear combination of the two constituent polymers,[40,41] although similar to the 3:1 diblock[37] polymer it appears that the enhanced backbone planarity and elongated chain of the fluorinated block is partially inhibiting the ordering of the non-fluorinated block in this 1:1 copolymer.

Table 1. Molecular weights and physical properties of P3OT, P3OT-*b*-F-P3OT, P3OT-*alt*-F-P3OT, and F-P3OT.

Polymer	M_n [kDa][a)]	M_w [kDa][a)]	T_c [°C]	T_m [°C]
P3OT	26	33	155	198
P3OT-*b*-F-P3OT	49	78	214	256
P3OT-*alt*-F-P3OT	64	88	199	244
F-P3OT	54	98	226	262

[a)]Measured by GPC against polystyrene standards in chlorobenzene at 80 °C except for F-P3OT, which was measured in 1,2,4-trichlorobenzene at 140 °C.

The decreasing trend in peak absorption value with increasing fluorination (Figure 1) may be expected to have a similar impact on the refractive index properties, following the usual Kramers–Kronig arguments.[42] As a preliminary investigation, we have modeled the measured specular reflection recorded from the thin-film samples (**Figure 2**), concentrating on the spectral region beyond the main absorption band (i.e., >700 nm). Employing a Cauchy-type description for the refractive indices of each material (Table S1, Supporting Information) does indeed suggest that the refractive index reduces upon increasing fluorination (inset of Figure 2).

Further influence to the extent of backbone fluorination on optoelectronic properties is evident from the measured work functions from polymer thin-film samples, listed in **Table 2**. Consistent with our previous report on the homopolymers, a stabilization of around 0.3 eV was observed upon fluorination.[34] P3OT-*alt*-F-P3OT exhibits an intermediate work function, close to halfway between the two homopolymers. Similar behavior was reported for an alternating thiophene–thiazole copolymer and an all-thiophene system where 3-hexylthiophene and 3-(2-ethylhexyl)thiophene were randomly copolymerized.[44,45] Conversely, P3OT-*b*-F-P3OT has a work function closer to that of the readily ionized P3OT. The phenomena of block copolymers displaying the work function of the most easily ionized block have previously been reported for polythiophene derivatives.[46,47] We note, however, that in the case of P3OT-*b*-F-P3OT, the work function is still 0.1 eV higher than P3OT.

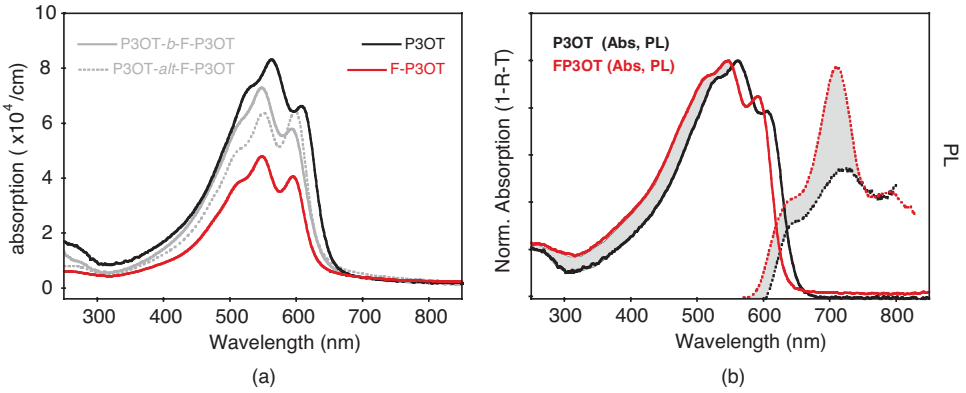

Figure 1. Spectral properties. a) Absorption spectra of the polymers in a thin-film format. b) Absorbance (solid line) and emission spectra (dotted line) from P3OT and F-P3OT thin films. A clear blue shift is evident for the F-P3OT spectra in comparison to P3OT.

2.3. Density Functional Theory (DFT) Calculations

DFT calculations on hexameric thiophene analogues were employed to predict the effect of fluorination on the dipole moment of the repeat units and, therefore, potentially on the dielectric constant of the polymer. Our calculations are based on the favored transoid conformation of the thiophene–thiophene bond since recent studies demonstrate that this is lower in energy compared with the cisoid.[34,36]

We observe that fluorination of the backbone leads to a large increase in the dipole moment (**Figure 3**; Figure S4, Supporting Information). Indeed, P3OT has a small dipole moment of 0.37 D along the backbone, but upon fluorination, this is increased to 7.72 D and remains largely directed along the backbone. Alternating the fluorination, while also increasing the dipole moment to 4.55 D, leads to a significant proportion of the dipole pointing away from the backbone. Translating these calculated values into a macroscopic property such as the dielectric constant is awkward since a number of factors come into play, such as the orientation of the repeat unit dipoles, their nanoscale ordering, and the projected alignment to the electric field. Nevertheless, a clear trend emerges that suggests increasing the backbone fluorination should lead to an increased dielectric constant, on the understanding that the materials all have a similar microstructure.

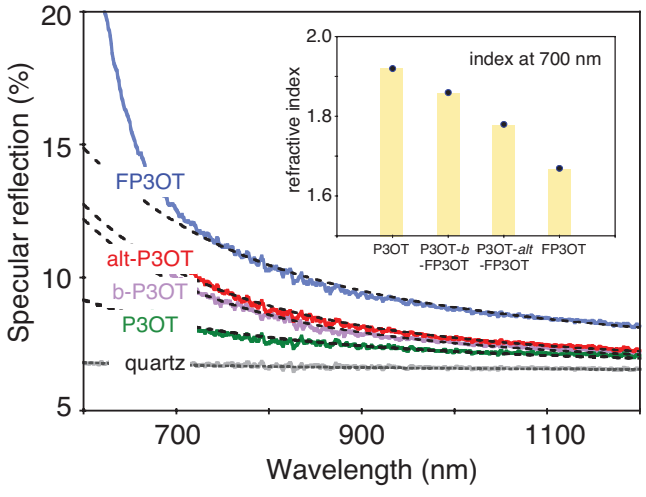

Figure 2. Specular reflection measured for the polymer thin films in the spectral region of low absorption. Superimposed (dotted lines) are calculated spectra assuming a Cauchy dispersion (Table S1, Supporting Information) for the refractive index. (inset) Illustrates the refractive index for the materials at wavelength of 700 nm.

2.4. Dielectric Constant

Capacitance–voltage (*C*–*V*) characteristics of metal–insulator–semiconductor diodes were measured to extract the low-frequency dielectric constant of the materials.[43,48–50] The devices, based on a p-type semiconductor (Si^{++}), include the thin-film polymer layers as part of the insulating region in addition to a native SiO_2 layer. In the usual nomenclature, we refer to the structure as a metal–oxide-semiconductor (MOS) capacitor structure (**Figure 4**; Figure S5, Supporting Information). The extracted dielectric constants (ε_r) of the polymers show that, compared with the reference material P3OT, increasing backbone fluorination increases ε_r for all cases (Figure 4b). In particular, full fluorination leads to a near doubling of the dielectric constant, i.e., from 2.71 to 4.82 for P3OT and F-P3OT, respectively. We note the value of ε_r for P3OT, obtained from our MOS structures, was in good agreement with a value of 2.84 obtained from a metal–insulator–metal (MIM) architecture

Table 2. Summary of calculated ground-state dipole moments (μ_g), the extracted dielectric constant (ε) and the work function measured by SKP and referenced against HOPG.

Polymer	μ_g [D]	ε_r [100 Hz]	Work function [eV]
			(±0.01)
P3OT	0.37	2.71	4.37
P3OT-*b*-F-P3OT	3.02	3.97	4.48
P3OT-*alt*-F-P3OT	4.55	4.30	4.58
F-P3OT	7.72	4.82	4.71

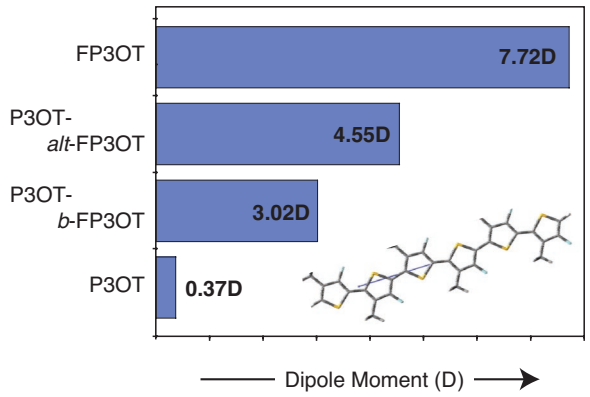

Figure 3. Calculated ground-state dipole moments based on hexameric thiophene analogues illustrating the increase in dipole moment with fluorination of the backbone. (inset) The minimum energy conformation and ground-state dipole moment for F-P3OT (see Figure S4, Supporting Information for more figures).

(Figure S6, Supporting Information). Both, however, are somewhat lower than the value of 3.24 previously reported for P3OT by ellipsometry.[50] The increase in ε_r upon fluorination reflects the trend observed in quinoxaline-based conjugated polymers and further suggests the dielectric constant of conjugated polymers respond differently to fluorination when compared with nonconjugated polymers.[4,11] At present, it is unclear from our results whether this difference can be assigned solely to the increased dipole moment, as predicted by DFT calculations, or if nanoscale ordering, and other microstructure effects (e.g., crystallite dipoles) are at play, as found for P(VDF-TrFE-CFE) and related high dielectric polymers.[19] In the case of these polyethylene-based fluorinated polymers, the anisotropy in crystalline domains resulting from the introduction of different comonomers is exploited. F-P3OT has indeed been reported to frustrate crystallization and has shorter coherence lengths in both the lamellar and π–π stacking directions than P3OT, which may indicate some differences in crystalline domains.[34]

The block copolymer, P3OT-*b*-F-P3OT, exhibits a dielectric constant that is close to the average of ε_{P3OT} and $\varepsilon_{F\text{-}P3OT}$, at 3.97, whereas the alternating copolymer, P3OT-*alt*-F-P3OT, recorded a dielectric constant approaching the fully fluorinated homopolymer. The latter case appears in line with previous reports, involving polyphenylene vinylene (PPV) copolymers with alkyl and ethylene glycol sidechains, where the alternating copolymers take on intermediate ε values of the two homopolymers.[20] The contrasting results obtained from the alternating and block copolymers confirm that the pattern of fluorination along a polymer chain has an influence. Despite the earlier perceived difficulties (and reservations) with directly translating DFT results, it is gratifying to note that of the two copolymer materials, the predicted dipole moment for the alternating copolymer was expected to be larger than the block copolymer, which is indeed the case with the dielectric constant. In fact, the overall trend in predicted dipole moment faithfully mirrors the trend observed with the measured dielectric constant (Table 2).

3. Conclusions

The ability to modify the electrical properties of semiconducting polymers, such as the dielectric constant, through chemical modification offers great promise and opportunities in many application areas. In this contribution, we have reported the synthesis of two novel copolymers based on partially fluorinated P3OT to probe the effect fluorination has on the dielectric constant, as well as the influence the pattern of fluorination can have on such properties. Through measurements of the low-frequency dielectric constant (ε) in MOS devices, we find that fluorination of only half of the thiophene units leads to a significant increase in the dielectric constant, i.e., from 2.7 for P3OT to 3.97 in a block copolymer configuration, and 4.3 for an alternating configuration. Full fluorination leads to an even larger increase to 4.8. The fact that both the alternating and block copolymers show substantial increases in ε compared with P3OT confirm that backbone fluorination is a useful tool for increasing the dielectric constant of semiconducting polymers. Deconvolving the factors that lie behind such an increase is difficult—nevertheless, we find a strong qualitative link between the calculated dipole moments and the measured dielectric constant—which correctly reproduce the increasing order. Inevitably the details and differences of microstructure undoubtedly play a significant

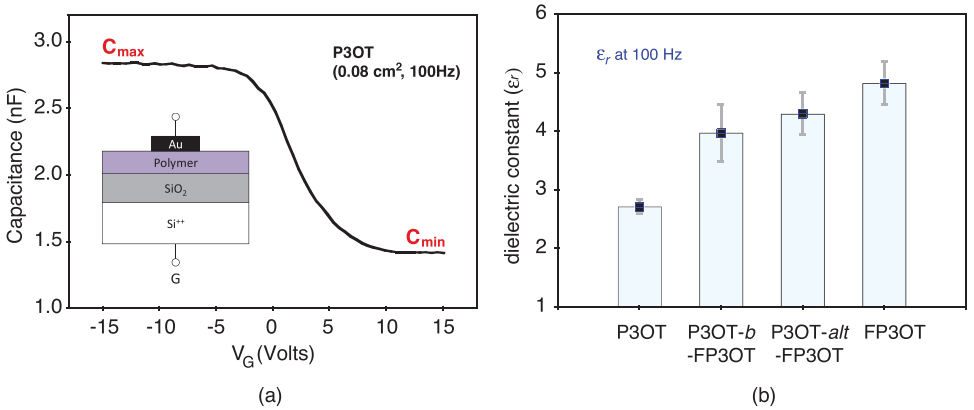

Figure 4. a) Capacitance–voltage response of a MOS device (see inset) featuring the typical accumulation and depletion regimes. b) The extracted dielectric constant of the polymers, obtained from the C_{min} value capacitance (data shown for 100 Hz).

role, as indeed highlighted from the absorption spectra and the degree of intrachain coupling between the two copolymers. Further studies, perhaps specifically targeting the microstructure of these polymers and the corresponding blends, would prove useful to elucidate the origin of the increase in ε_r. Finally, of particular interest would be the subsequent performance of these polymers in photovoltaic devices.[51]

4. Experimental Section

Materials: Reagents and chemicals were purchased from commercial sources such as Sigma-Aldrich and Acros etc. unless otherwise stated. 2,5-dibromo-3-fluoro-4-octylthiophene (3) was synthesized according to previously reported procedures.[34] All reactions were carried out under argon using solvents and reagents as commercially supplied, unless otherwise stated.

*Synthesis of 2-Tributylstannyl-4-Octylthiophene (**2**)*: In a dry 2-neck flask, 3-octylthiophene (1.80 g, 9.17 mmol) was dissolved in dry tetrahydrofuran (THF, 20 mL) THF (20 mL) and cooled to −78 °C. Lithium diisopropylamide (5.05 mL, 2.0 M in THF/heptane/ethylbenzene) was then added dropwise, and the resulting solution was stirred at −78 °C for 2 h, after which tributyltin chloride (4.48 g, 13.76 mmol) was slowly added. The reaction mixture was further stirred at −78 °C for 2 h, before being warmed to room temperature, and finally poured into water (100 mL) and extracted with hexane (3 × 50 mL). The organic extracts were washed with water (3 × 100 mL), and acetonitrile (4 × 50 mL), and dried over sodium sulfite. The solvent was removed in vacuo to yield the crude product (**2**) as pale yellow oil, which was used for the next step without further purification. ^{1}H NMR (400 MHz, $CDCl_3$) δ 7.19 (s, 1H), 6.96 (s, 1H), 2.65 (t, J = 7.6 Hz, 2H), 1.63–1.46 (m, 8H), 1.39–1.26 (m, 16H), 1.14–1.07 (m, 6H), 0.88 (m, 12H).

*Synthesis of 2-Bromo-3-Fluoro-4-Octylthiophene (**4**)*: In a dry 20 mL microwave vial, 2,5-dibromo-3-fluoro-4-octylthiophene (1.48 g, 3.98 mmol) was dissolved in dry THF (10 mL), and to the stirred solution isopropylmagnesium chloride lithium chloride complex (3.06 mL, 1.3 M in THF) was added dropwise. After 30 min, methanol (2 mL) was added, and after a further 5 min, the reaction mixture was poured into saturated ammonium chloride (50 mL) and extracted with hexane (3 × 50 mL). The organic extracts were dried over magnesium sulfate and the solvent removed in vacuo to yield the crude product (**4**) as a light brown oil (1.125 g, 96%). ^{1}H NMR (400 MHz, $CDCl_3$) δ 6.62 (d, J = 1.7 Hz, 1H), 2.51 (t, J = 7.6 Hz, 2H), 1.59–1.46 (m, 2H), 1.39–1.15 (m, 10H), 0.88 (t, J = 7.0 Hz, 3H). ^{13}C NMR(101 MHz, $CDCl_3$) δ 155.3 (d, J = 262.7 Hz), 131.8 (d, J = 24.1 Hz), 109.1 (d, J = 10.0 Hz), 103.2 (d, J = 21.2 Hz), 32.1, 29.5, 29.4, 29.4, 28.8, 26.8, 22.8, and 14.3. ^{19}F NMR (377 MHz, $CDCl_3$) δ −125.59. HRMS (EI)$^+$ calculated for $C_{12}H_{18}SBrF$: 292.0297, found: 292.0305.

*Synthesis of 4-Fluoro-3,4′-Dioctyl-2,2′-Bithiophene (**5**)*: In a dry 20 mL microwave vial, **3** (2.15g, 4.43 mmol), **4** (1.00 g, 3.41 mmol), bis(dibenzylideneacetone)palladium (97 mg, 5 mol%), and tris(*o*-tolyl) phosphine (103 mg, 10 mol%) were added, and the vial was evacuated and backfilled with Ar three times, before degassed toluene (10 mL) was added. The reaction mixture was degassed by bubbling argon, and then heated to 150 °C for 2 h in a microwave reactor. The reaction mixture was then passed through a silica plug using hexane as eluent, and the solvent was removed in vacuo. The resulting oil was purified by reverse phase chromatography using methanol as eluent to yield the product as a colorless oil (730 mg, 53%). ^{1}H NMR (400 MHz, $CDCl_3$, δ): 6.95 (d, J = 1.4 Hz, 1H), 6.93–6.89 (m, 1H), 6.58 (d, J = 1.4 Hz, 1H), 2.72–2.64 (m, 2H), 2.64–2.57 (m, 2H), 1.72–1.49 (m, 4H), 1.42–1.19 (m, 20H), 0.88 (m, 6H), ^{13}C NMR (100 MHz, $CDCl_3$, δ): 156.59 (d, J = 259.1 Hz), 143.70, 135.65, 130.54 (d, J = 8.1 Hz), 128.32 (d, J = 23.1 Hz), 127.17, 120.49, 101.22 (d, J = 20.9 Hz), 31.90, 30.48, 30.43, 29.74, 29.50, 29.45, 29.35, 29.30, 29.26, 25.97, 22.70, 14.13, ^{19}F NMR (377 MHz, $CDCl_3$, δ): −127.10 (s), EIMS m/z (%): 408 (30) [M$^+$], HRMS (ESI) m/z: [M$^+$] calculated for $C_{24}H_{37}FS_2$, 408.2321, found: 408.2311.

*Synthesis of 5,5′-Dibromo-4-Fluoro-3,4′-Dioctyl-2,2′-Bithiophene (**6**)*: In 100 mL flask covered in aluminium foil, **5** (700 mg, 1.71 mmol) was dissolved in chloroform (10 mL), and to the solution was added *N*-bromosuccinimide (641 mg, 3.60 mmol). The reaction was stirred for 12 h and then extracted with water (50 mL), 1 M sodium hydroxide solution (20 mL), and the solvent was removed in vacuo. The resulting oil was passed through a silica plug using hexane as eluent, and the solvent was removed in vacuo to yield the product as a colorless oil (902 mg, 94%). ^{1}H NMR (400 MHz, $CDCl_3$, δ): 6.76 (s, 1H), 2.64 (d, J = 8.0 Hz, 2H), 2.55 (d, J = 7.8 Hz, 2H), 1.67–1.47 (m, 4H), 1.40–1.20 (m, 20H), 0.88 (t, J = 6.6 Hz, 6H), ^{13}C NMR (100 MHz, $CDCl_3$, δ): 154.65 (d, J = 261.5 Hz), 142.70, 134.29, 129.24, 129.16 (d, J = 29.9 Hz), 127.18, 109.91 (d, J = 15.5 Hz), 89.98 (d, J = 22.3 Hz), 31.88, 29.63, 29.51, 29.37, 29.24, 29.20, 26.31, 22.68, 14.13, ^{19}F NMR (377 MHz, $CDCl_3$, δ): −125.09 (s), EIMS m/z (%): 564 (10) [M$^+$], HRMS (ESI) m/z: [M-Br_2]$^+$ calculated for $C_{24}H_{35}FS_2$, 406.2164, found: 406.2147.

Typical Procedure for Synthesis of Grignard Monomer: In a dry 100 mL Schlenk tube, isopropylmagnesium chloride lithium chloride complex (4.10 mL, 1.3 M in THF) was added dropwise to a solution of 2,5-dibromo-3-octylthiophene (1.89 g, 5.33 mmol) in dry THF (25 mL). After 30 min, the resulting Grignard monomer solution (0.18 M in THF) was ready for use.

Synthesis of Poly(3-Octylthiophene-2,5-Diyl) (P3OT): Grignard solution freshly prepared from 2,5-dibromo-3-octylthiophene (29.1 mL, 0.18 M solution in THF) was added via cannula to a dry 100 mL 2-neck flask under Ar containing dichloro(1,3-bis(diphenylphosphino)propane)nickel (28.9 mg, 1 mol%) and fitted with a reflux condenser. The reaction was then refluxed for 12 h, before being poured into methanol (200 mL) acidified with a few drops of concentrated HCl. The precipitate was filtered through a cellulose thimble, and the solid purified by Soxhlet extraction with methanol, acetone, hexane (in each case until the extracting solvent was colorless), and finally extracted with chloroform, before being precipitated into methanol and filtered. The solid was dried under vacuum to give P3OT (740 mg, 72%). M_n 26 kDa, M_w 33 kDa. ^{1}H NMR (400 MHz, $CDCl_3$,δ): 6.98 (1 H, s), 2.93–2.48 (2 H, m), 1.76–1.62 (2 H, m), 1.45–1.20 (10 H, m), 0.94–0.80 (3 H, m). Anal. calculated for $C_{12}H_{18}S$, C 74.17, H 9.34, found: C 74.03, H 9.43.

Synthesis of Poly(3-Fluoro-4-Octylthiophene-2,5-Diyl) (F-P3OT): In a dry 20 mL microwave vial, 2,5-dibromo-3-fluoro-4-octylthiophene (1.00 g, 2.69 mmol) was dissolved in dry THF (17 mL), and to the stirred solution, isopropylmagnesium chloride lithium chloride complex (1.97 mL, 1.3 M in THF) was added dropwise. After 30 min, a suspension of dichloro(1,3-bis(diphenylphosphino)propane)nickel (7.3 mg, 0.5 mol%) in dry THF (0.7 mL) was added to the Grignard monomer solution, and the resulting solution was stirred at 70 °C for 12 h, before being poured into methanol (200 mL) acidified with a few drops of concentrated HCl. The precipitate was filtered through a glass thimble, and the solid purified by Soxhlet extraction with methanol, acetone, hexane, chloroform (in each case until the extracting solvent was colorless), and finally extracted with chlorobenzene, before being precipitated into methanol and filtered. The solid was dried under vacuum to give F-P3OT (420 mg, 73%). M_n 54 kDa, M_w 98 kDa. ^{1}H NMR (400 MHz, TCE-d_2, 403 K, δ): 2.82 (t, J = 7.8 Hz, 2H), 1.74 (t, J = 7.6, 2H), 1.61–1.35 (m, 14H), 1.02–0.92 (m, 3H), ^{19}F NMR (376 MHz, TCE-d_2, 403 K, δ): −122.95 (s), Anal. calculated for $C_{12}H_{17}FS$, C 67.88, H 8.07, found: C 67.76, H 7.99. (Inconsistency in ^{1}H integration attributed to residual H_2O in solvent.)

Synthesis of Poly(3-Octylthiophene-Block-3-Fluoro-4-Octylthiophene) (P3OT-b-F-P3OT): In a dry 2–5 mL microwave vial charged with dichloro(1,3-bis(diphenylphosphino)propane)nickel (2.7 mg, 0.5 mol%) was added Grignard solution freshly prepared from 2,5-dibromo-3-octylthiophene (2.67 mL, 0.28 M in THF), and the reaction mixture was stirred at 40 °C for 1 h, after which Grignard solution freshly prepared from 2,5-dibromo-3-fluoro-4-octylthiophene (0.89 mL, 0.28 M) was added, and the reaction heated to 70 °C for 12 h before being poured into methanol (200 mL) acidified with a few drops of concentrated HCl. The precipitate was filtered through a cellulose thimble, and the solid purified by Soxhlet extraction with methanol, acetone, and hexane (in each case until the extracting solvent was colorless). In order to determine if substantial amounts of P3OT homopolymer still remained,

a differential scanning calorimetry (DSC) was run on a sample, and after confirmation that this was indeed the case, the solid was further washed with dichloromethane and finally extracted with chloroform, before being precipitated into methanol and filtered. The solid was dried under vacuum to give P3OT-*b*-F-P3OT (50 mg, 25%). M_n 49 kDa, M_w 78 kDa. ^{1}H NMR (400 MHz, TCE-d_2, 403 K, δ): 7.06 (s, 1H), 2.96–2.61 (m, 4H), 1.89–1.63 (m, 4H), 1.56–1.31 (m, 21H), 1.06–0.89 (m, 6H), ^{19}F NMR (376 MHz, TCE-d_2, 403 K, δ): –122.49 (s). Anal. calculated for $C_{24}H_{35}FS_2$, C 70.89, H 8.68, found: C 70.75, H 8.75. (Inconsistency in ^{1}H integration attributed to residual H_2O in solvent.)

Synthesis of Poly(4-Fluoro-3,4′-Dioctyl-2,2′-Bithiophene-5,5′Diyl) (P3OT-alt-F-P3OT): In a dry 20 mL microwave vial, **6** (750 g, 1.33 mmol) was dissolved in dry THF (17 mL), and to the stirred solution isopropylmagnesium chloride lithium chloride complex (1.00 mL, 1.3 M in THF) was added dropwise. After 1 h, a suspension of dichloro(1,3-bis(diphenylphosphino)propane)nickel (10.8 mg, 1.5 mol%) in dry THF (1 mL) was added to the Grignard monomer solution, and the resulting solution was stirred at 70 °C for 5 h, before being poured into methanol (200 mL) acidified with a few drops of concentrated HCl. The precipitate was filtered through a cellulose thimble, and the solid purified by Soxhlet extraction with methanol, acetone, hexane, and chloroform (in each case until the extracting solvent was colorless). The residual polymer was dissolved in chlorobenzene, precipitated into methanol, and filtered. The solid was dried under vacuum to give P3OT-*alt*-F-P3OT (313 mg, 58%). M_n 64 kDa, M_w 88 kDa. ^{1}H NMR (400 MHz, TCE-d_2, δ): 7.11 (s, 1H), 2.93–2.74 (m, 4H), 1.88–1.70 (m, 4H), 1.57–1.31 (m, 22H), 1.02–0.89 (m, 6H), ^{19}F NMR (376 MHz, TCE-d_2, 403 K, δ): –122.59 (s). Anal. calculated for $C_{24}H_{35}FS_2$, C 70.89, H 8.68, found: C 70.77, H 8.73. (Inconsistency in ^{1}H integration attributed to residual H_2O in solvent.)

Material Characterization: ^{1}H, ^{19}F, and ^{13}C NMR spectra were recorded on a Bruker AV-400 (400 MHz), using the residual solvent resonance of chloroform-*d* or 1,1,2,2-tetrachloroethane-*d*[2] and are given in ppm. Microwave experiments were performed in a Biotage initiator V 2.3. Number-average (M_n) and weight-average (M_w) molecular weights were determined by using an Agilent Technologies 1200 series GPC running in chlorobenzene at 80 °C, using two PL mixed B columns in series, and calibrated against narrow-polydispersity polystyrene standards. Due to poor solubility, M_n and M_w of F-P3OT was measured in 1,2,4-trichlorobenzene at 140 °C using a Polymer Laboratories PL-220 high-temperature GPC instrument calibrated against polystyrene standards. Electrospray mass spectrometry was performed with a Thermo Electron Corp. DSQII mass spectrometer. DSC measurements, using ≈3 mg of material, were conducted under nitrogen at scan rate of 10 °C min^{-1} with a TA DSC-Q20 instrument.

DFT Calculations: These were carried out using the B3LYP hybrid functional and the 6–31 g(d) basis set in the GAUSSIAN09 software package.[52] Alkyl chains were replaced with a methyl group to simplify calculations and reduce computational time.

Optical Characterization: Transmission and specular reflection spectra of polymer films on quartz substrates were acquired in the UV–vis and near infrared regions (220–1400 nm) using a Shimadzu UV-2600 spectrometer fitted with ISR-2600Plus integrating sphere option.

Scanning Kelvin Probe (SKP) measurements were performed at room temperature under ambient conditions by using an SKP5050 system from KP Technology Ltd. Samples were prepared by spin coating on ITO glass substrates, and work function values were calculated by averaging the last 500 measurement points of each data set (2000 points in total). For reference, a highly oriented pyrolytic graphite (HOPG) sample, with a nominal work function of 4.480 eV was used. The measurement uncertainty was calculated as the square of the quadratic sum of errors (the standard deviation) of both HOPG and sample data sets.

Device Fabrication: For the MOS device configuration, thin films of the polymers were spin coated from hot (≈150 °C) solution in 1,2,4-trichlorobenzene (5 mg mL^{-1}) at 3000 rpm for 2 min onto hot Si^{++} substrates with a 100 nm thick native SiO_2 layer (except P3OT, which was spun on room temperature substrates due to issues with dewetting). Metal top contacts (Au, thickness 40 nm, areas between 0.01 and 0.16 cm^2) were subsequently deposited by thermal evaporation (rate 0.1 nm s^{-1}) using shadow masks. Additional MIM devices, comprising P3OT as the insulator, were prepared by spin coating a film (thickness 141 ± 5 nm) onto a glass substrate where bottom Au electrodes were previously deposited. Top Au contacts were then evaporated on the P3OT film, thus defining metal/polymer/metal structures. All polymer thickness values were measured using a Dektak 150 surface profilometer by taking several measurements for each film and calculating the average and std. deviation.

Dielectric Characterization: A Schlumberger SI 1260 impedance/gain phase analyzer was used for the determination of the dielectric constants of the polymers by impedance spectroscopy. Capacitance–frequency (*C–f*) and Capacitance–Voltage (*C–V*) measurements were performed in the 10–10^6 Hz frequency range and with applied bias varied between –15 and +15 V. The capacitance of the MOS structure depends on the bias voltage applied, which influence the charge accumulation or depletion at the interface between the polymer and the oxide. The maximum capacitance, obtained in the accumulation regime at high negative bias for a p-type semiconductor, is determined exclusively by the oxide layer

$$C_{max} = C_{SiO_2} = \frac{\varepsilon_0 \varepsilon_{SiO_2} A}{d_{SiO_2}} \quad (1)$$

where A is the device area, ε_0 the vacuum permittivity, ε_{SiO_2} the dielectric constant of the insulator and d_{SiO_2} its thickness. The minimum capacitance is obtained when the polymer film is fully depleted at positive bias. The depleted polymer layer acts as a capacitor in series with the oxide layer, hence the total capacitance is

$$\frac{1}{C_{min}} = \frac{1}{C_{SiO_2}} + \frac{1}{C_{polymer}} \quad (2)$$

The capacitance for the polymer, $C_{polymer,}$ can therefore be extracted as

$$C_{polymer} = \frac{C_{SiO_2} C_{min}}{C_{SiO_2} - C_{min}} = \frac{\varepsilon_0 \varepsilon_{polymer} A}{d_{polymer}} \quad (3)$$

to obtain an estimate for the dielectric constant, $\varepsilon_{polymer,}$ of the polymer.[34–36]

Supporting Information

Supporting Information is available from the Wiley Online Library or from the author.

Acknowledgements

The authors would like to acknowledge the EPSRC Centre for Doctoral Training in Plastic Electronic Materials (EP/L016702/1, EP/G037515/1), the British Council (Grant No. 337323), and the Leverhulme Trust for financial support.

Conflict of Interest

The authors declare no conflict of interest.

Keywords

block copolymers, conjugated polymers, dielectric constant, fluorination

Received: August 11, 2017
Revised: September 19, 2017
Published online: November 27, 2017

[1] Q.-D. Ling, D.-J. Liaw, C. Zhu, D. S.-H. Chan, E.-T. Kang, K.-G. Neoh, *Prog. Polym. Sci.* **2008**, *33*, 917.
[2] H. Sirringhaus, *Adv. Mater.* **2014**, *26*, 1319.
[3] L. J. A. Koster, S. E. Shaheen, J. C. Hummelen, *Adv. Energy Mater.* **2012**, *2*, 1246.
[4] Y. Lu, Z. Xiao, Y. Yuan, H. Wu, Z. An, Y. Hou, C. Gao, J. Huang, *J. Mater. Chem. C* **2013**, *1*, 630.
[5] G. Zhang, T. M. Clarke, A. J. Mozer, *J. Phys. Chem. C* **2016**, *120*, 7033.
[6] S. Chen, S.-W. Tsang, T.-H. Lai, J. R. Reynolds, F. So, *Adv. Mater.* **2014**, *26*, 6125.
[7] J. E. Donaghey, A. Armin, P. L. Burn, P. Meredith, *Chem. Commun.* **2015**, *51*, 14115.
[8] X. Chen, Z. Zhang, Z. Ding, J. Liu, L. Wang, *Angew. Chem., Int. Ed. Engl.* **2016**, *55*, 10376.
[9] T. M. Clarke, J. R. Durrant, *Chem. Rev.* **2010**, *110*, 6736.
[10] N. Cho, C. W. Schlenker, K. M. Knesting, P. Koelsch, H.-L. Yip, D. S. Ginger, A. K. Y. Jen, *Adv. Energy Mater.* **2014**, *4*, 1301857.
[11] P. Yang, M. Yuan, D. F. Zeigler, S. E. Watkins, J. A. Lee, C. K. Luscombe, *J. Mater. Chem. C* **2014**, *2*, 3278.
[12] B. Yang, J. Cox, Y. Yuan, F. Guo, J. Huang, *Appl. Phys. Lett.* **2011**, *99*, 133302.
[13] S. Torabi, F. Jahani, I. Van Severen, C. Kanimozhi, S. Patil, R. W. A. Havenith, R. C. Chiechi, L. Lutsen, D. J. M. Vanderzande, T. J. Cleij, J. C. Hummelen, L. J. A. Koster, *Adv. Funct. Mater.* **2015**, *25*, 150.
[14] C. Deibel, T. Strobel, V. Dyakonov, *Adv. Mater.* **2010**, *22*, 4097.
[15] I. Constantinou, X. Yi, N. T. Shewmon, E. D. Klump, C. Peng, S. Garakyaraghi, C. K. Lo, J. R. Reynolds, F. N. Castellano, F. So, *Adv. Energy Mater.* **2017**, *7*, 1601947.
[16] J.-G. Liu, M. Ueda, *J. Mater. Chem.* **2009**, *19*, 8907.
[17] W. Groh, A. Zimmermann, *Macromolecules* **1991**, *24*, 6660.
[18] L. Yang, X. Li, E. Allahyarov, P. L. Taylor, Q. M. Zhang, L. Zhu, *Polymer* **2013**, *54*, 1709.
[19] L. Zhu, *J. Phys. Chem. Lett.* **2014**, *5*, 3677.
[20] M. Breselge, I. Van Severen, L. Lutsen, P. Adriaensens, J. Manca, D. Vanderzande, T. Cleij, *Thin Solid Films* **2006**, *511*, 328.
[21] S. Zhang, Z. Zhang, J. Liu, L. Wang, *Adv. Funct. Mater.* **2016**, *26*, 6107.
[22] A. Armin, D. M. Stoltzfus, J. E. Donaghey, A. J. Clulow, R. C. R. Nagiri, P. L. Burn, I. R. Gentle, P. Meredith, *J. Mater. Chem. C* **2017**, *5*, 3736.
[23] S. Y. Leblebici, T. L. Chen, P. Olalde-Velasco, W. Yang, B. Ma, *ACS Appl. Mater. Interfaces* **2013**, *5*, 10105.
[24] M. Guo, X. Yan, Y. Kwon, T. Hayakawa, M.-A. Kakimoto, T. Goodson, *J. Am. Chem. Soc.* **2006**, *128*, 14820.
[25] M. Guo, X. Yan, T. Goodson, *Adv. Mater.* **2008**, *20*, 4167.
[26] M. Guo, T. Hayakawa, M. Kakimoto, T. Goodson, *J. Phys. Chem. B* **2011**, *115*, 13419.
[27] J. T. Bendler, C. A. Edmondson, M. C. Wintersgill, D. A. Boyles, T. S. Filipova, J. J. Fontanella, *Eur. Polym. J.* **2012**, *48*, 830.
[28] F. Meyer, *Prog. Polym. Sci.* **2015**, *47*, 70.
[29] N. Leclerc, P. Chávez, O. Ibraikulov, T. Heiser, P. Lévêque, *Polymers* **2016**, *8*, 11.
[30] S. Xiao, Q. Zhang, W. You, *Adv. Mater.* **2017**, *29*, 1601391.
[31] A. C. Stuart, J. R. Tumbleston, H. Zhou, W. Li, S. Liu, H. Ade, W. You, *J. Am. Chem. Soc.* **2013**, *135*, 1806.
[32] B. Carsten, J. M. Szarko, H. J. Son, W. Wang, L. Lu, F. He, B. S. Rolczynski, S. J. Lou, L. X. Chen, L. Yu, *J. Am. Chem. Soc.* **2011**, *133*, 20468.
[33] B. Carsten, J. M. Szarko, L. Lu, H. J. Son, F. He, Y. Y. Botros, L. X. Chen, L. Yu, *Macromolecules* **2012**, *45*, 6390.
[34] Z. Fei, P. Boufflet, S. Wood, J. Wade, J. Moriarty, E. Gann, E. L. Ratcliff, C. R. McNeill, H. Sirringhaus, J.-S. Kim, M. Heeney, *J. Am. Chem. Soc.* **2015**, *137*, 6866.
[35] R. S. Loewe, S. M. Khersonsky, R. D. McCullough, *Adv. Mater.* **1999**, *11*, 250.
[36] J. T. Blaskovits, T. Bura, S. Beaupré, S. A. Lopez, C. Roy, J. de Goes Soares, A. Oh, J. Quinn, Y. Li, A. Aspuru-Guzik, M. Leclerc, *Macromolecules* **2017**, *50*, 162.
[37] P. Boufflet, S. Wood, J. Wade, Z. Fei, J.-S. Kim, M. Heeney, *Beilstein J. Org. Chem.* **2016**, *12*, 2150.
[38] Z. Hu, R. T. Haws, Z. Fei, P. Boufflet, M. Heeney, P. J. Rossky, D. A. Vanden Bout, *Proc. Natl. Acad. Sci. U. S. A.* **2017**, *114*, 5113.
[39] F. C. Spano, C. Silva, *Annu. Rev. Phys. Chem.* **2014**, *65*, 477.
[40] J. Hollinger, A. A. Jahnke, N. Coombs, D. S. Seferos, *J. Am. Chem. Soc.* **2010**, *132*, 8546.
[41] E. F. Palermo, A. J. McNeil, *Macromolecules* **2012**, *45*, 5948.
[42] P. N. Stavrinou, G. Ryu, M. Campoy-Quiles, D. D. C. Bradley, *J. Phys.: Condens. Matter* **2007**, *19*, 466107.
[43] G. Bovo, I. Braunlich, W. R. Caseri, N. Stingelin, T. D. Anthopoulos, K. G. Sandeman, D. D. C. Bradley, P. N. Stavrinou, *J. Mater. Chem. C* **2016**, *4*, 6240.
[44] H. Bronstein, M. Hurhangee, E. C. Fregoso, D. Beatrup, Y. W. Soon, Z. Huang, A. Hadipour, P. S. Tuladhar, S. Rossbauer, E.-H. Sohn, S. Shoaee, S. D. Dimitrov, J. M. Frost, R. S. Ashraf, T. Kirchartz, S. E. Watkins, K. Song, T. Anthopoulos, J. Nelson, B. P. Rand, J. R. Durrant, I. McCulloch, *Chem. Mater.* **2013**, *25*, 4239.
[45] B. Burkhart, P. P. Khlyabich, B. C. Thompson, *Macromolecules* **2012**, *45*, 3740.
[46] D. Gao, J. Hollinger, D. S. Seferos, *ACS Nano* **2012**, *6*, 7114.
[47] D. Izuhara, T. M. Swager, *Macromolecules* **2011**, *44*, 2678.
[48] E. J. Meijer, A. V. G. Mangnus, B. H. Huisman, G. W. 't Hooft, D. M. de Leeuw, T. M. Klapwijk, *Synth. Methods* **2004**, *142*, 53.
[49] E. J. Meijer, A. V. G. Mangnus, C. M. Hart, D. M. d. Leeuw, T. M. Klapwijk, *Appl. Phys. Lett.* **2001**, *78*, 3902.
[50] S. Scheinert, W. Schliefke, *Synth. Methods* **2003**, *139*, 501.
[51] J.-P. Sun, J. T. Blaskovits, T. Bura, S. Beaupré, M. Leclerc, I. G. Hill, *Org. Electron.* **2017**, *50*, 115.
[52] M. J. Frisch, G. W. Trucks, H. B. Schlegel, G. E. Scuseria, M. A. Robb, J. R. Cheeseman, G. Scalmani, V. Barone, B. Mennucci, G. A. Petersson, H. Nakatsuji, M. Caricato, X. Li, H. P. Hratchian, A. F. Izmaylov, J. Bloino, G. Zheng, J. L. Sonnenberg, M. Hada, M. Ehara, K. Toyota, R. Fukuda, J. Hasegawa, M. Ishida, T. Nakajima, Y. Honda, O. Kitao, H. Nakai, T. Vreven, J. A. Montgomery Jr., J. E. Peralta, F. Ogliaro, M. J. Bearpark, J. Heyd, E. N. Brothers, K. N. Kudin, V. N. Staroverov, R. Kobayashi, J. Normand, K. Raghavachari, A. P. Rendell, J. C. Burant, S. S. Iyengar, J. Tomasi, M. Cossi, N. Rega, N. J. Millam, M. Klene, J. E. Knox, J. B. Cross, V. Bakken, C. Adamo, J. Jaramillo, R. Gomperts, R. E. Stratmann, O. Yazyev, A. J. Austin, R. Cammi, C. Pomelli, J. W. Ochterski, R. L. Martin, K. Morokuma, V. G. Zakrzewski, G. A. Voth, P. Salvador, J. J. Dannenberg, S. Dapprich, A. D. Daniels, Ö. Farkas, J. B. Foresman, J. V. Ortiz, J. Cioslowski, D. J. Fox, Gaussian 09, Revision C.01. Wallinford, CT **2009**.